

Effect of the Functionalization of the Axial Phthalocyanine Ligands on the Energy Transfer in QD-based Donor–Acceptor Pairs

Smita Dayal, Jun Li, Ying-Syi Li, Hongqiao Wu, Anna C. S. Samia, Malcolm E. Kenney* and Clemens Burda*

Center for Chemical Dynamics and Nanomaterials Research, Department of Chemistry, Case Western Reserve University, Cleveland, OH

Received 20 May 2007, accepted 22 August 2007, DOI: 10.1111/j.1751-1097.2007.00227.x

ABSTRACT

This study examines the electronic coupling between quantum dots (QDs) and molecules on their surfaces as a function of the modality of their interaction. As a probe, the energy transfer (ET) between CdSe QDs and phthalocyanines (Pcs) was monitored and evaluated with regard to the functionalization of the axial phthalocyanine ligand, bulkiness of the functional group bridging the QD donor and Pc acceptor, and the number of the functionalized axial ligands. New silicon PCs and their conjugates with CdSe QDs were synthesized. The ET efficiency and kinetics were studied by steady state and femtosecond time-resolved absorption spectroscopy. We observed a decrease in ET efficiency with the increase in functional group bulkiness, which could be explained by increasing steric hindrance between the ET pair. In addition, a higher ET efficiency was observed for amino and thiol functionalized Pcs compared to Pcs without functional group on the axial alkyl chain.

INTRODUCTION

Much of the current semiconductor quantum dot (QD) research is focused on the properties of QDs in solution and on various factors with regard to the conjugation of QDs to various ligands such as antibodies, drug molecules, markers, *etc.* (1–6). QDs show potential for applications in diagnostics and therapy (7), especially imaging (8–10) and photodynamic therapy (PDT) (11,12). QD-based PDT utilizes energy transfer (ET) between donor–acceptor (DA) systems (1,2,6). It has been shown that II–VI semiconductor QD work as energy donors in PDT conjugates (11,12). CdSe QDs offer various advantages over conventional organic fluorescent molecules such as high extinction coefficients, continuous absorption spectra, size-tunable emission wavelengths, resistance to photobleaching upon continuous irradiation, and long-lived excited states. The surface chemistry of both the QDs and the acceptor molecules along with the geometry of the molecules plays a decisive role in the ET mechanism and therefore for its efficiency. Conjugates of CdSe QDs with phthalocyanines (Pcs) have been under study for PDT (6,11). Here, the QDs serve as the donors and the Pcs as the

acceptors. These conjugates can be excited in a very broad excitation window as the QDs exhibit continuous absorption spectra. Previous studies (6) on QD donors and Pc acceptor molecules revealed some of the contributions of surface-related factors. Thus an increase in ET efficiency with an increase in the length of the DA linker chain was observed when the rest of variables, such as QD emission wavelength and functionalization of the axial group on the Pc, were kept constant. The increase in ET efficiency was explained by an increase in the interdigitization of the linker chain into the QD capping layer. The sum of the above studies indicates the complexity of the ET phenomenon through surface or interface-related states.

In this report, we examine the influence of the Pc functional groups (binding modality) and their bulkiness (steric hindrance) on the ET efficiency using steady-state and femtosecond (fs) time-resolved visible-light spectroscopy. For this study four new Pcs with different binding functional groups were synthesized and conjugated to QDs. Optical properties of CdSe QDs are influenced by interactions with their environment. Better surface passivation with various capping ligands such as amines (13) and with higher band-gap semiconductors (14–16) result in higher emission quantum yields of the QD. Here, we present the influence of the chemical functionality of axial ligands in Pc molecules on the DA interactions, probed by the ET efficiency and dynamics.

MATERIALS AND METHODS

Synthesis of CdSe QDs and conjugates. CdSe QDs were synthesized following the method of Peng and Peng (17). In brief, 0.0510 g CdO (STREM), 3.75 g trioctylphosphine oxide (Aldrich) and 2 g hexadecyl amine (Aldrich) were heated under argon gas at 320°C to obtain a colorless Cd precursor. A selenium precursor was obtained by dissolving 0.0410 g Se powder (STREM) in 2 g trioctylphosphine (Fluka). This was injected into CdO precursor at 270°C. The resulting QDs were allowed to grow at 250°C. The growth of QDs was quenched by injecting them into anhydrous cold toluene. The QD samples were washed twice by precipitating them with anhydrous methanol and then redissolving them in toluene.

Synthesis of phthalocyanines. $\text{HOSiPcOSi}(\text{CH}_3)_2(\text{CH}_2)_3\text{N}(\text{CH}_3)_2$, Pc 4; $\text{SiPcOSi}[(\text{CH}_3)_2(\text{CH}_2)_3\text{N}(\text{CH}_3)_2]_2$, Pc 12; and $\text{HOSiPcOSi}[(\text{CH}_3)_2(\text{CH}_2)_3\text{N}(\text{CH}_2)_n\text{H}]_n$, $n = 2–5$, Pc 34, Pc 121, Pc 25 and Pc 122. Syntheses of Pc 4 (18–20), Pc 12 (18–22), Pc 34 (23) and Pc 25 (23) have been reported earlier. Syntheses of Pc 121 and Pc 122 will be reported elsewhere (J. C. Berlin, G. Hao, Y-S. Li, M. E. Kenney and M. A. J. Rodgers, unpublished data).

*Corresponding authors email: mekq@case.edu (Malcolm E. Kenney), burda@case.edu (Clemens Burda)

© 2007 The Authors. Journal Compilation. The American Society of Photobiology 0031-8655/08

CH₃OSi(CH₃)₂(CH₂)₃SH, 1. Under Ar, a 0°C solution of 3-mercaptopropyltrimethoxysilane (8.5 g) and tetrahydrofuran (50 mL) was treated dropwise with a CH₃MgCl-tetrahydrofuran solution (50 mL). The reaction mixture was stirred for 1 h and then treated dropwise with CH₃OH (40 mL), both being done at low temperature (0°C), diluted with a tetrahydrofuran-diethyl ether solution (1:8, 90 mL), and filtered. The solid was washed (diethyl ether), and the washings and filtrate were combined and concentrated by rotary evaporation at room temperature. The concentrate was distilled (60 torr, 90–110°C) and weighed (3.8 g, 54%). ¹H NMR (C₆D₆): δ 3.21 (s, 3H, OCH₃), 2.24 (q, 2H, Si(CH₂)₂CH₂), 1.49 (m, 2H, SiCH₂CH₂), 1.14 (t, 1H, SH), 0.47 (m, 2H, SiCH₂), 0.04 (s, 6H, SiCH₃).

1 is a colorless liquid. It is soluble in CH₂Cl₂, dimethylformamide, toluene and hexanes.

SiPc[OSi(CH₃)₂(CH₂)₃SH]₂, Pc 93, 2. Under Ar, a mixture of SiPc(OH)₂ (135 mg), silane 1 (1.60 g), and pyridine (80 mL) was distilled (5 mL of distillate) for 1 h, and evaporated to dryness by rotary evaporation (30°C). The solid was chromatographed (basic-Al₂O₃ III, CH₂Cl₂-ethyl acetate solution, 5:1), air-dried, and weighed (190 mg, 96%). UV-Vis (toluene) λ_{max}, nm: 669. ¹H NMR (C₆D₆): δ 9.72 (m, 8H, 1, 4-Pc H), 7.87 (m, 8H, 2, 3-Pc H), 0.91 (q, 4H, Si(CH₂)₂CH₂), 0.39 (t, 2H, SH), -1.02 (m, 4H, SiCH₂CH₂), -2.22 (t, 4H, SiCH₂), -2.68 (s, 12H, SiCH₃). ¹³C NMR (CDCl₃): δ 148.9 (5-Pc C), 136.3 (4a-Pc C), 131.1 (2, 3-Pc C), 123.9 (1, 4-Pc C), 27.1 (Si(CH₂)₂CH₂), 27.0 (SiCH₂CH₂), 15.3 (SiCH₂), -3.2 (SiCH₃).

2 is a blue solid. It is soluble in CH₂Cl₂, dimethylformamide and toluene, and insoluble in hexanes.

HOSiPcOSi(CH₃)₂(CH₂)₃SH, Pc 219, 3. A mixture of phthalocyanine 2 (114 mg) and a solution of trichloroacetic acid (150 mg) in CH₂Cl₂ (100 mL) was stirred at room temperature for 1.5 h, treated with pyridine (20 mL) and then H₂O (100 mL), and separated. The aqueous portion of the reaction product was washed (CH₂Cl₂), and the washings and the organic portion of the reaction product were combined and concentrated by rotary evaporation (room temperature). The concentrate was passed down an Al₂O₃ column (basic-Al₂O₃ V, CH₂Cl₂-ethyl acetate solution, 10:1), and evaporated to dryness by rotary evaporation (room temperature). The solid was washed (acetonitrile), air-dried and weighed (52 mg, 50%). UV-Vis (toluene) λ_{max}, nm: 680. ¹H NMR (C₆D₆): δ 9.67 (m, 8H, 1, 4-Pc H), 7.84 (m, 8H, 2, 3-Pc H), 0.90 (q, 2H, Si(CH₂)₂CH₂), 0.36 (t, 1H, SH), -1.00 (m, 2H, SiCH₂CH₂), -2.19 (t, 2H, SiCH₂), -2.64 (s, 6H, SiCH₃). ¹³C NMR (CDCl₃): 149.9 (5-Pc C), 135.8 (4a-Pc, C), 131.6 (2, 3-Pc, C), 124.2 (1, 4-Pc, C), 27.0 (Si(CH₂)₂CH₂), 26.8 (SiCH₂CH₂), 15.0 (SiCH₂), -3.2 (SiCH₃). HRMS-MALDI (*m/z*): [M-OH]⁺ calcd for C₃₇H₂₉N₈OSSi₂, 689.1724; found 689.1690.

3 is a blue solid. It is soluble in CH₂Cl₂, dimethylformamide and toluene, and insoluble in hexanes.

HOSi(CH₃)₂(CH₂)₃CH₃, 4. *n*-Butyldimethylchlorosilane (5.0 mL) was added to a cool (ice bath) solution of H₂O (1.0 mL), N(C₂H₅)₃ (5.0 mL) and ether (50 mL), and the mixture was stirred for 1 h at room temperature and filtered. The filtrate was concentrated to an oil by rotary evaporation (30°C), and the oil was weighed (3.09 g, 81%). ¹H NMR (C₆D₆): δ 1.28 (m, 4H, SiCH₂(CH₂)₂), 0.86 (t, 3H, Si(CH₂)₃CH₃), 0.48 (m, 2H, SiCH₂), 0.01 (s, 6H, SiCH₃).

4 is a colorless oil.

SiPc[OSi(CH₃)₂(CH₂)₃CH₃]₂, Pc 109, 5. A mixture of silanol 4 (257 mg) and a suspension of SiPc(OH)₂ (150 mg) and pyridine (70 mL) that had been dried by distillation (9 mL of distillate) was distilled (34 mL of distillate) for 2 h, and the residual was evaporated to dryness by rotary evaporation (40°C). The solid was chromatographed (Al₂O₃ I, toluene), washed (hexanes), vacuum-dried (60°C), and weighed (60 mg, 29%). UV-Vis (toluene) λ_{max}, nm: 668. ¹H NMR (C₆D₆): δ 9.73 (m, 8H, 1, 4-Pc H), 7.88 (m, 8H, 2, 3-Pc H), 0.12 (t, 6H, Si(CH₂)₃CH₃), -0.08 (m, 4H, Si(CH₂)₂CH₂), -1.14 (m, 4H, SiCH₂CH₂), -2.10 (m, 4H, SiCH₂), -2.62 (s, 12H, SiCH₃). HRMS-FAB (*m/z*): [M]⁺ calcd for C₄₄H₄₆N₈O₂Si₃, 802.3052; found 802.3068, 802.3056.

5 is a blue solid. It is soluble in CH₂Cl₂, dimethylformamide and toluene, and slightly soluble in hexanes.

CH₃OSi(CH₃)₂(CH₂)₃C(CH₃)₃, 6. A solution of 4, 4-dimethyl-1-pentene (2.01 g), dimethylchlorosilane (4.0 mL) and platinum-divinyltetramethyldisiloxane complex in xylene (Gelest, 2.1–2.4% Pt in xylenes, 0.1 mL) in a pressure tube was warmed (60°C) for 2 days, purged with Ar at elevated temperature (60°C), treated with CH₃OH (5 mL) and concentrated to an oil by rotary evaporation (30°C). The

oil was distilled (40 torr, 83–92°C) and weighed (1.23 g, 32%). ¹NMR (CDCl₃): δ 3.40 (s, 3H, CH₃O), 1.32 (m, 2H, Si(CH₂)₂CH₂), 1.20 (m, 2H, SiCH₂CH₂), 0.87 (s, 9H, Si(CH₂)₃CCH₃), 0.78 (m, 2H, SiCH₂), 0.08 (s, 6H, SiCH₃).

6 is colorless oil.

SiPc[OSi(CH₃)₂(CH₂)₃C(CH₃)₃]₂, Pc 110, 7. A mixture of silanol 6 (316 mg) and a suspension of SiPc(OH)₂ (150 mg) and pyridine (70 mL) that had been dried by distillation (4 mL of distillate) was distilled (14 mL of distillate) for 2 h, and the residual was evaporated to dryness by rotary evaporation (40°C). The solid was chromatographed (Al₂O₃ III, hexanes-CH₂Cl₂ solution, 4:1), vacuum-dried (60°C) and weighed (187 mg, 81%). UV-Vis (toluene) λ_{max}, nm: 668. ¹H NMR (300 MHz, C₆D₆): δ 9.72 (m, 8H, 1, 4-Pc H), 7.89 (m, 8H, 2, 3-Pc H), 0.42 (s, 18H, Si(CH₂)₃CCH₃), 0.11 (m, 4H, Si(CH₂)₂CH₂), -1.11 (m, 4H, SiCH₂CH₂), -2.09 (m, 4H, SiCH₂), -2.60 (s, 12H, SiCH₃). HRMS-FAB (*m/z*): [M]⁺ calcd for C₅₀H₅₈N₈O₂Si₃, 886.3991; found 886.3985, 886.3999.

7 is a blue solid. It is soluble in CH₂Cl₂, dimethylformamide and toluene, and insoluble in hexanes.

Synthesis of QD-Pc conjugates. The Pcs (18–24) were dissolved in anhydrous toluene and mixed with QD solutions. QD and Pc concentrations of 5 × 10⁻⁵ and 8 × 10⁻⁵ M were used to obtain high ET efficiency and to keep Pc self-quenching low.

Photophysical studies. The synthesized QDs and conjugates were studied by steady-state absorption (Varian Cary 50) and fluorescence (Varian Eclipse fluorescence spectrophotometer) spectroscopy. A 500 nm wavelength light excitation was used for all the spectroscopic studies. It should be emphasized that one can excite the QDs exclusively if 500 nm light is used because the Pcs do not appreciably absorb at this wavelength. The Pc emission peak observed near 675 nm is therefore due solely to ET from the photoexcited QDs. QDs with an emission at 625 nm were used so as to have sufficient spectral overlap for good ET with the Pcs used, all of which have very similar absorption profiles.

For the study of ET dynamics, pure QDs and QD-conjugates were investigated by fs time-resolved laser spectroscopy after 24 h of conjugation time. It was found that 24 h is the optimum time for conjugation (6), when maximum quenching of the QD emission occurs while at the same time the Pc fluorescence could be detected. Broadband fs-laser pulses were used to probe the dynamics at the fs time scale between 450 and 750 nm. The laser setup has been discussed previously (25,26). For the fs measurements, 2 mm quartz cuvettes were used. All experiments were carried out at room temperature. Absorption spectra were collected before and after the time-resolved measurements. No changes in the absorption spectra were detected.

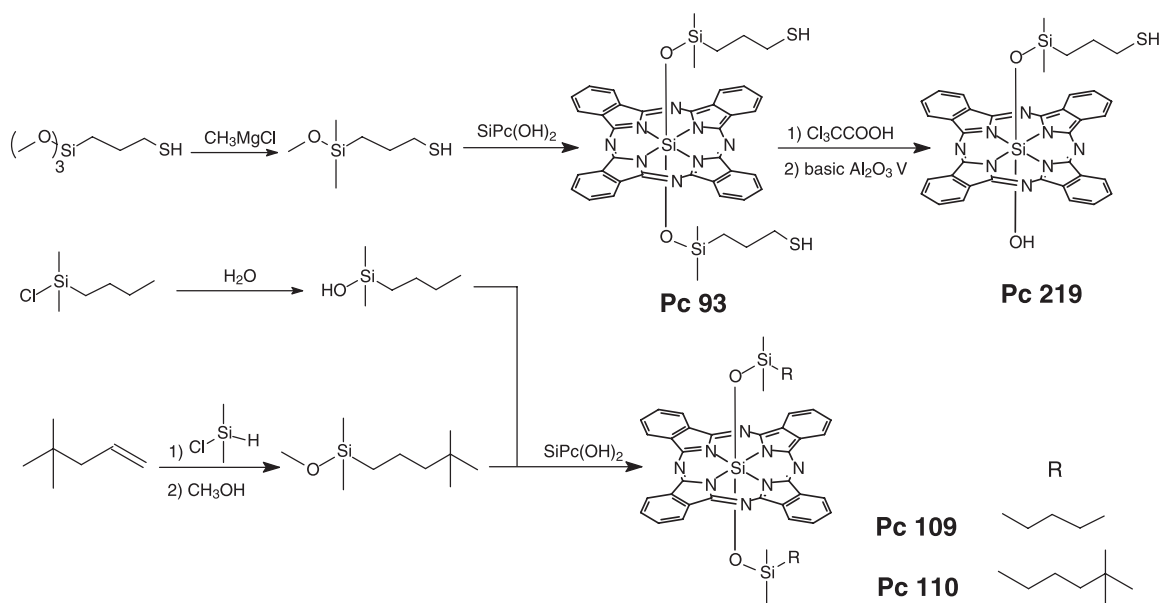
RESULTS AND DISCUSSION

The synthesis of Pc 93, Pc 219, Pc 109 and Pc 110 is summarized in Scheme 1. The reactions used to prepare the precursors for Pc 219, Pc 109 and Pc 110 and those used to prepare the compounds themselves follow reactions developed earlier for similar molecules (18–20). The molecules used in this study are depicted in Fig. 1.

The effects of axial group functionalization on ET

To study the effects of functionalization of the siloxy ligands of the Pcs and those of the number (one or two) of functionalized siloxy ligands on ET efficiency, conjugates of the QDs with various Pcs were studied. The terminology used for the parts of the axial ligands is explained in Fig. 2.

Effect of axial ligand functionalization on ET-amino vs thiol functions. The effect of axial ligand functionalization was studied by conjugating Pc 4 and Pc 219 to CdSe QDs. Pc 4 has a dimethylamino group as axial ligand function while Pc 219 has a thiol function (Fig. 1). Figure 3a shows the steady-state absorption and emission spectra of the QDs and their conjugates. A higher quenching efficiency of QD emission



Scheme 1. Synthesis scheme for Pc 93, Pc 219, Pc 109 and Pc 110.

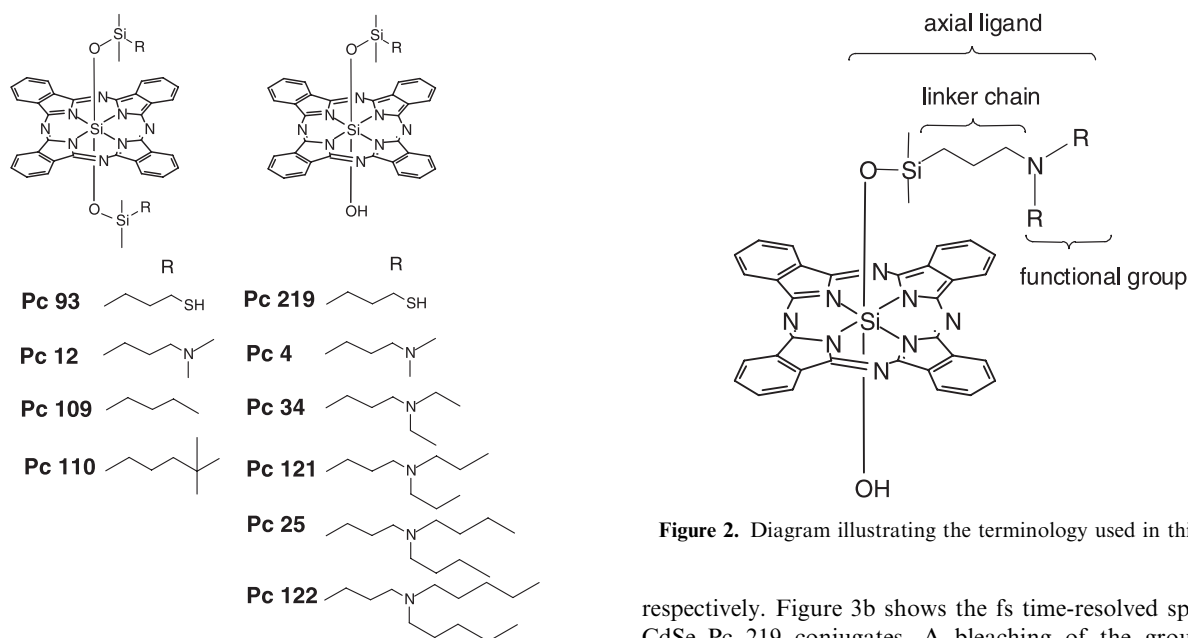


Figure 1. Structures of the phthalocyanines used in this study.

was observed for Pc 4, while a bigger peak corresponding to Pc emission was observed for Pc 219. This difference can be explained partially by a slightly higher fluorescence quantum yield of Pc 219 compared to that of Pc 4. In addition, the absorption spectrum of Pc 219 shows a slight redshift compared to that of Pc 4 and therefore the overlap integral for Pc 219 is not as effective with CdSe QDs as for Pc 4. It should be noted that the ET is a function of donor quantum yield and not of acceptor quantum yield and can be calculated by the decrease in the integrated donor emission in the presence and absence of the donor using Eq. (1).

As Fig. 3a indicates, the integrated emission intensities reveal ET efficiencies of 75% and 54% for Pc 4 and Pc 219,

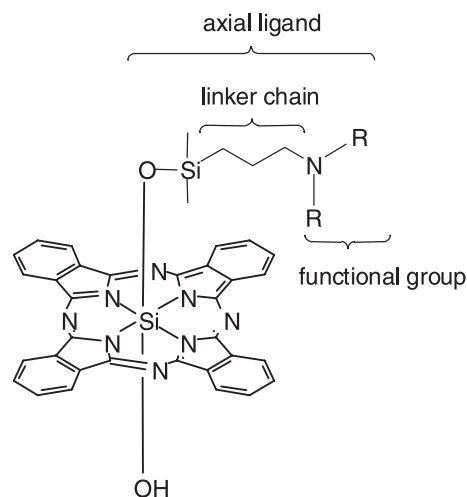


Figure 2. Diagram illustrating the terminology used in this study.

respectively. Figure 3b shows the fs time-resolved spectra for CdSe–Pc 219 conjugates. A bleaching of the ground state absorption of the QDs was observed at 610 nm followed by a bleach signal at 682 nm corresponding to Pc 219 excitation. The 610 nm bleach signal decays over time and results in the build up of the 682 nm signal due to the ET. Respective kinetics observed at the QD bleach maxima are shown in the inset of Fig. 3b. The observed kinetic traces were fitted with mono-exponential fits in the time frame of interest (350 ps).

The steady-state ET efficiency $\phi_{ET}^{St.State}$ was calculated with Eq. (1) (27):

$$\phi_{ET}^{St.State} = 1 - \frac{I_{DA}}{I_D} \quad (1)$$

where I_D and I_{DA} are the relative intensities of the donor emission in the absence and presence of the acceptor.

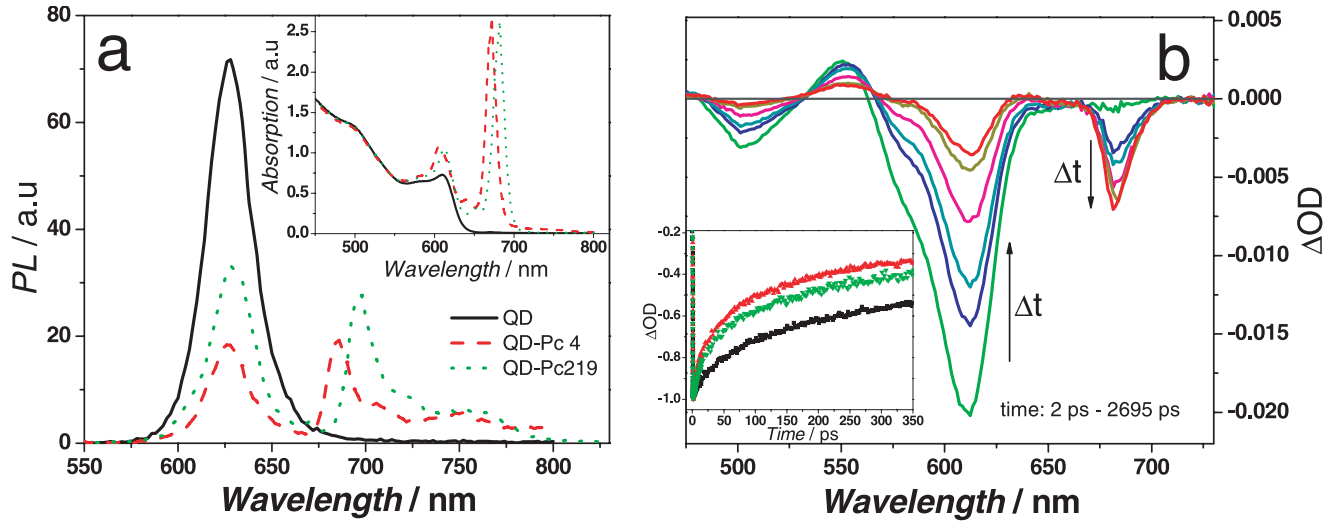


Figure 3. (a) Steady-state emission spectra of CdSe QDs and their conjugates with Pc 4 and Pc 219 with a dimethylamino and thiol functional group, respectively. The inset shows the absorption spectra. (b) Femtosecond spectra of conjugates of CdSe QDs with Pc 219, showing two consecutive bleach signals at 610 and 682 nm corresponding to QD and Pc excitation, respectively. The inset shows the normalized decay dynamics observed at the QD bleach wavelength (612 nm) for pure QDs and their conjugates with Pc 4 and Pc 219. 500 nm excitation wavelength was used for the exclusive excitation of the QDs.

The transfer efficiency ϕ_{ET}^{Kin} , based on the lifetimes, was calculated from the lifetime measurements of the donor, in the absence (τ_D) and presence (τ_{DA}) of the acceptor as shown in Eq. (2) (27).

$$\phi_{ET}^{Kin} = 1 - \frac{\tau_{DA}}{\tau_D} \quad (2)$$

Steady-state and time-resolved ET efficiencies are summarized in Table 1. The observed differences in efficiencies between different Pcs can be explained by the varying interactions between the various Pc functional groups and the QD surface.

Effect of axial group functionalization on ET-amino vs alkyl groups. We also studied the ET between QD donors and Pc acceptors having methyl (Pc 109), *tert*-butyl (Pc 110) and dimethylamino terminated axial ligands (Pc 12). Here, the ligands with methyl and *tert*-butyl terminations have nonpolar terminations and interact with the QDs only through Van der Waals interactions. If one assumes a termination-dependent ET process, all these conjugates should show different ET efficiencies as the interaction between various Pc functional groups and the CdSe capping ligands is expected to be different. The fact that the number of methylene groups in the

Table 1. Decay constants obtained by mono-exponential fitting of the measured kinetic traces.

	Decay time/ps τ_{QD}^{QD}	ET efficiency ϕ_{ET}^{Kin}	SS ET efficiency $\phi_{ET}^{St.State}$	ϕ_{PL}^{Pc}
QDs	93.7	0	0	
QD-Pc 4	59.79	0.36	0.75	1
QD-Pc 219	61.85	0.34	0.54	1.07
QD-Pc 109	67.70	0.28	0.17	0.978
QD-Pc 110	71.66	0.23	0.08	0.953
QD-Pc 12	62.73	0.33	0.78	0.386

ET = energy transfer; QD = quantum dot; Pc = phthalocyanine.

linker chain was kept constant is important as it is known from previous work (6) that the length of the linker chain plays a significant role for ET efficiencies.

Figure 4a shows the steady-state emission spectra of the pure QDs and their conjugates with Pc 109, Pc 110 and Pc 12. Respective absorption spectra are shown in the inset of Fig. 4a. It is easily seen that for the conjugates of QDs with Pc 109 and Pc 110 no significant steady-state ET was observed (although the Pc 109 conjugate is slightly more efficient than the Pc 110 conjugate) while QD-Pc 12 conjugate shows a very efficient ET. According to the PL-quenching measurements, the Pc 109 and Pc 110 conjugates show an ET efficiency of <20% compared with 78% for the Pc 12 conjugate.

The same phenomenon was indicated by the time-resolved measurements shown in Fig. 4b. QD conjugates with Pc 109 and Pc 110 showed only a small acceleration in the QD excitation decay kinetics while QD-Pc 12 showed a significant acceleration. These observations can be explained on the basis of the chain terminations. Here, Pc 109 and Pc 110 are terminated by simple aliphatic groups and therefore the ET occurs only through space or possibly through bonds due to the interdigitation of the alkyl chain into the TOPO capping layer of the QD, and indeed a very low ET efficiency was observed. But in case of Pc 12 as energy acceptor, one finds an increased ET efficiency due to the increased interaction between the amino groups and the QD surface.

Effect of one vs two axial ligands. Here, the ET efficiencies between QDs and Pc 4 and Pc 12, which have one vs two dimethylamino axial ligands, respectively, are compared. Figure 5a shows the steady-state absorption and emission spectra monitored for the QDs and their conjugates. Higher PL-quenching was observed for QD emission when they were conjugated with Pc 12. Pc 12 conjugate shows an efficiency of 78% compared with 75% for Pc 4 conjugates. Femtosecond time-resolved spectra for Pc 12 conjugates are shown in Fig. 5b and the inset shows the decay kinetics for QD bleach

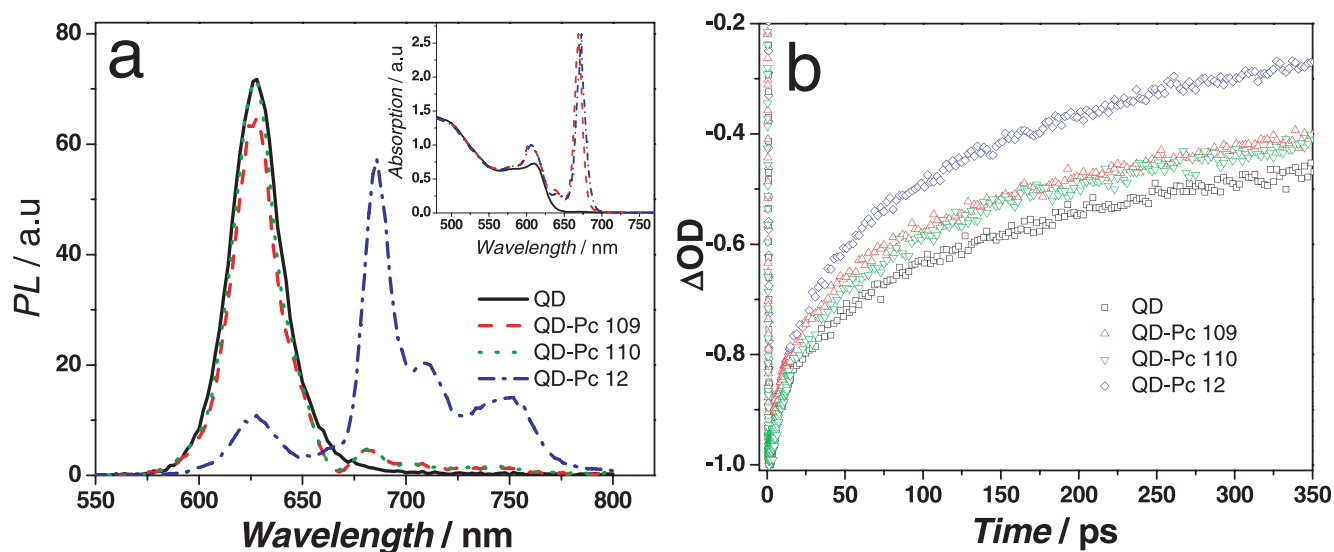


Figure 4. (a) Steady-state emission spectra of CdSe QDs and their conjugates with Pc 109, Pc 110 and Pc 12. The inset shows the respective absorption spectra. (b) Normalized time-resolved kinetic traces for CdSe QDs and their conjugates with Pc 109, Pc 110 and Pc 12 observed at the QD bleach extrema at 610 nm.

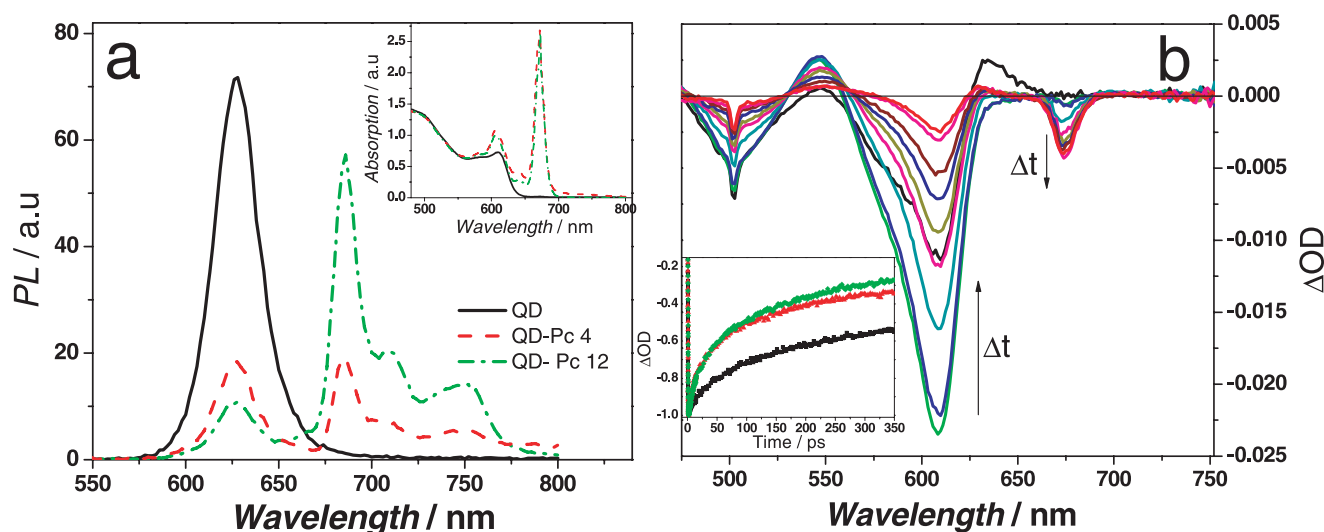


Figure 5. (a) Steady-state emission spectra of CdSe QDs and their conjugates with Pc 4 and Pc 12. The inset shows the absorption spectra. (b) Femtosecond time-resolved spectra of CdSe QD conjugates with Pc 12 show the 610 nm bleach signal, corresponding to QD excitation, and build up of the Pc ground state bleaching at 673 nm. The inset shows the normalized time-resolved kinetic traces for CdSe QDs and conjugates with Pc 4 and Pc 12 observed at 610 nm.

maxima at 610 nm. A better ET efficiency for the Pc 12 conjugate compared with the Pc 4 conjugate was observed by both steady state and time-resolved measurements. This can be explained by the fact that Pc 12 has two dimethylamino functional groups compared with one for Pc 4 and therefore shows a better binding, either due to a chelating effect of the bis(dimethylamino) Pc or simply due to the two-fold increased availability of the amino ligand. Similarly, we also compared the ET efficiency of Pc 219 with that of Pc 93, which have one vs two thiol axial ligands, respectively. Again, a better ET efficiency was observed for Pc 93. These observations indicate that the number of functionalized groups in the investigated acceptor moieties plays another significant role for the ET

efficiency from QDs. This underlines the importance of choosing the appropriate linker chains in order to maximize ET efficiencies.

The effect of functional group bulkiness on the ET

Previous studies on Pc linker chain length showed a behavior where the ET efficiency increases with an increase in Pc linker chain length. This observation was explained by the better interdigitization of the longer phthalocyanine linker chains into the organic capping layer of QDs. In this context, we further studied the effect of functional group chain lengths in amino functionalized ligands on the ET by keeping the other

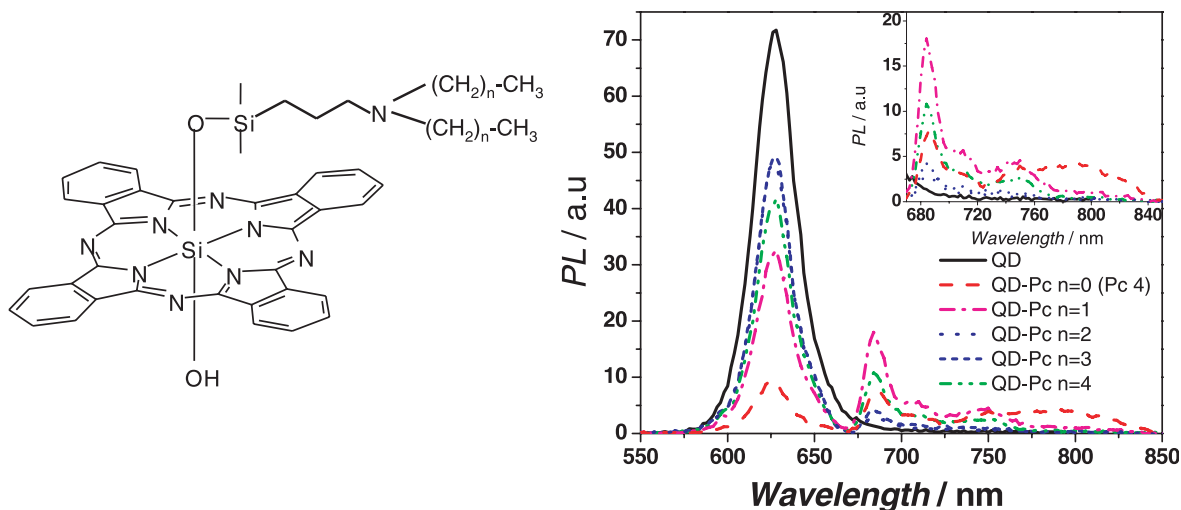


Figure 6. Structure of studied Pc molecules (Pc 4, Pc 34, Pc 121, Pc 25 and Pc 122) with variable terminal bulkiness (left) and steady-state emission spectra of CdSe QDs and their conjugates with Pcs of different functional group bulkiness (right). The inset shows a closer look of the Pc emission in the region of interest (660–850 nm).

variables, such as linker chain length and overlap integral (QD size) constant. All studied homologous Pcs (Pc 4, Pc 34, Pc 121, Pc 25 and Pc 122) have an axial ligand with three methylene groups in the linker chain between the silicon atom and the amine group (*i.e.* Pc-O-Si(CH₃)₂-(CH₂)₃-N((CH₂)_nMe)₂), as shown in Fig. 6. The amino groups vary from dimethylamino to dipentylamino (n varies between 0 and 4). Figure 6 shows the steady-state ET emission spectra for conjugates with different functional group chain lengths. The steady state and time-resolved ET efficiencies show the same trend, as shown in Fig. 7a,b. Pc 4, which has methyl groups as the functional group chain ($n = 0$) shows the maximum efficiency, and on increasing the number of -CH₂- groups in the functional group chain the ET efficiency decreases, as shown in Fig. 7. We observed the lowest ET efficiency for C₃H₁₁ functional group chains. Thus, the efficiency decreases with the bulkiness of the functional group chains. This can be

explained on the basis of less efficient interdigitization due to steric hindrance.

The measurements of the ET efficiency with time-resolved and steady-state spectroscopy could be used to evaluate the interactions between QD energy donors and molecular acceptors in QD-based ET pairs. As subsequent singlet oxygen generation from the excited Pc moiety will be a function of the ET efficiency, this information can be used to improve and optimize the application in PDT. In a broader picture, this study underlines that coupling drugs to QDs requires a rather detailed analysis of various parameters, such as the size of the used QDs, choice of the surface capping molecules, the bridging linker chain, the binding chemical functionality, involvement of QD surface states, *etc.* if one aims to optimize the interactions within the conjugate. This applies also to the increasingly used bio-conjugated QDs. We emphasize that in this report the QD conjugates were not studied in a

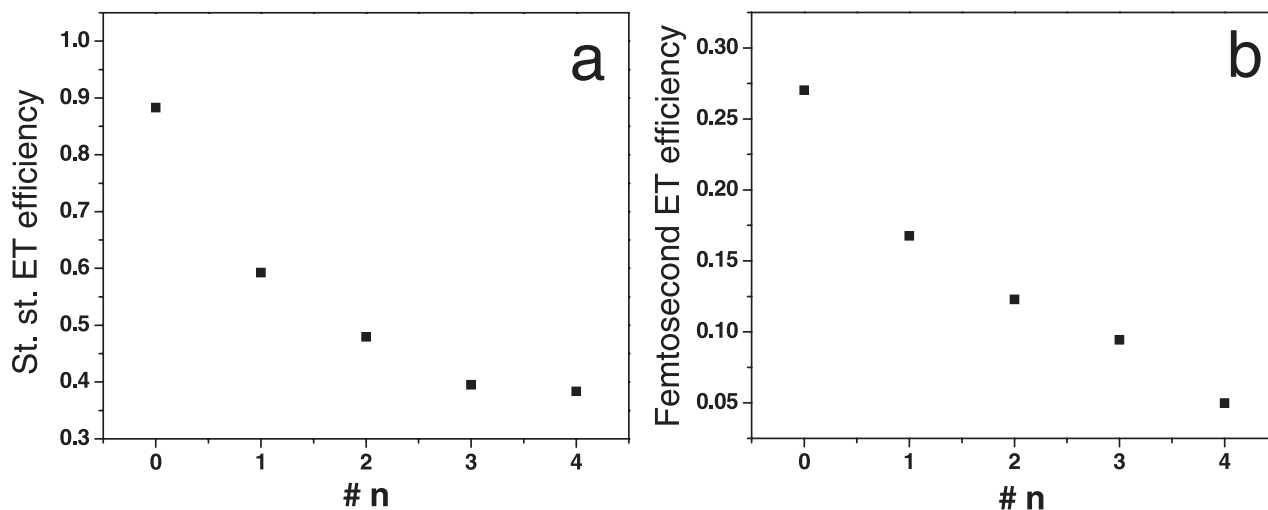


Figure 7. ET transfer efficiencies obtained from (a) steady state and (b) time-resolved spectroscopy, plotted for Pc functional group bulkiness in QD-Pc conjugates plotted as a function of terminal chain length (n = number of methylene groups).

cell-friendly medium. It rather presents an overall view of a QD-based DA system where the efficiency of the ET process can be increased and optimized by choosing the right molecular functionalities.

CONCLUSIONS

In conclusion, QDs are excellent energy donors and visible light sensitizers, which can be useful for many applications in various fields. The usefulness of visible light excited QDs is proportional to the electronic coupling between the QDs and the ligated energy acceptors. This study found that amines and thiols make almost equally good binding groups for attaching molecules to QDs. On the other hand, nonfunctionalized molecules couple significantly less, as quantified in the Results section (see also Table 1). We observed a decrease in ET efficiency with an increase in functional group bulkiness due to an increase in steric hindrance. We also observed a higher ET efficiency for the Pcs with two functionalized axial ligands compared with the Pcs with just one axial ligand. Therefore, functionalization of the acceptor group plays a significant role in affecting the efficiency and dynamics of the ET process.

Acknowledgement—C.B. and M.E.K. are grateful for the funding from BRTT, Ohio Board of Regents. C.B. gratefully acknowledges financial support from NSF (#CHE-0239688).

REFERENCES

- Goldman, E. R., E. D. Balighian, H. Mattoussi, M. K. Kuno, J. M. Mauro, P. T. Tran and G. P. Anderson (2003) Avidin: A natural bridge for quantum dot-antibody conjugates. *J. Am. Chem. Soc.* **124**, 6378–6382.
- Goldman, E. R., G. P. Anderson, P. T. Tran, H. Mattoussi, P. T. Charles and J. M. Mauro (2002) Conjugation of luminescent quantum dots with antibodies using an engineered adaptor protein to provide new reagents for fluoroimmunoassays. *Anal. Chem.* **124**, 841–847.
- Wu, X., H. Liu, J. Liu, K. N. Haley, J. A. Treadway, J. P. Larson, N. Ge, F. Peale and M. P. Bruchez (2003) Immunofluorescent labeling of cancer marker Her2 and other cellular targets with semiconductor quantum dots. *Nat. Biotechnol.* **21**, 41–46.
- Bruchez, M., Jr., M. Moronne, P. Gin, S. Weiss and A. P. Alivisatos (1998) Semiconductor nanocrystals as fluorescent biological labels. *Science* **281**, 2013–2016.
- Larson, D. R., W. R. Zipfel, R. M. Williams, S. W. Clark, M. P. Bruchez, F. W. Wise and W. W. Webb (2003) Water-soluble quantum dots for multiphoton fluorescence imaging in vivo. *Science* **300**, 1434–1436.
- Dayal, S., Y. B. Lou, A. C. S. Samia, J. C. Berlin, M. E. Kenney and C. Burda (2006) Observation of non-Förster-type energy-transfer behavior in quantum dots-phthalocyanine conjugates. *J. Am. Chem. Soc.* **128**, 13974–13975.
- Samia, A. C. S., S. Dayal and C. Burda (2006) Quantum dot-based energy transfer: Perspectives and potential for applications in photodynamic therapy. *Photochem. Photobiol.* **82**, 617–625.
- Jaiswal, J. K., H. Mattoussi, J. M. Mauro and S. M. Simon (2003) Long-term multiple color imaging of live cells using quantum dot bioconjugates. *Nat. Biotechnol.* **21**, 47–51.
- Derfus, A. M., W. C. W. Chan and S. N. Bhatia (2004) Intracellular delivery of quantum dots for live cell labeling and organelle tracking. *Adv. Mater.* **16**, 961–966.
- Gao, X., Y. Cui, R. M. Levenson, L. W. K. Chung and S. Nie (2004) In vivo cancer targeting and imaging with semiconductor quantum dots. *Nat. Biotechnol.* **22**, 969–976.
- Samia, A. C. S., X. Chen and C. Burda (2003) Semiconductor quantum dots for photodynamic therapy. *J. Am. Chem. Soc.* **125**, 15736–15737.
- Bakalova, R., Z. Ohba, Z. Zhelev, M. Ishikawa and Y. Baba (2004) Quantum dots as photosensitizers? *Nat. Biotechnol.* **22**, 1360–1361.
- Talapin, D. V., A. L. Rogach, A. Kornowski, M. Haase and H. Weller (2001) Highly luminescent monodisperse CdSe and CdSe/ZnS nanocrystals synthesized in a hexadecylamine-trioctylphosphine oxide-trioctylphosphine mixture. *Nano. Lett.* **1**, 207–211.
- Dabbousi, B. O., J. Rodriguez-Viejo, F. V. Mikulec, J. R. Heine, H. Mattoussi, R. Ober, K. F. Jensen and M. Bawendi (1997) (CdSe)ZnS core-shell quantum dots: Synthesis and characterization of a series of highly luminescent nanocrystallites. *J. Phys. Chem. B* **101**, 9463–9475.
- Kuno, M., J. K. Lee, B. O. Dabbousi, F. V. Mikulec and M. G. Bawendi (1997) The band edge luminescence of surface modified CdSe nanocrystallites: Probing the luminescing state. *J. Chem. Phys.* **106**, 9869–9882.
- Peng, X., M. C. Schlamp, A. Kadavanich and A. P. Alivisatos (1997) Epitaxial growth of highly luminescent CdSe/CdS core/shell nanocrystals with photostability and electronic accessibility. *J. Am. Chem. Soc.* **119**, 7019–7029.
- Peng, Z. A. and X. G. Peng (2001) Formation of high-quality CdTe, CdSe, and CdS nanocrystals using CdO as precursor. *J. Am. Chem. Soc.* **123**, 183–184.
- Oleinick, N. L., A. R. Antunez, M. E. Clay, B. D. Richter and M. E. Kenney (1993) New phthalocyanine photosensitizers for photodynamic therapy. *Photochem. Photobiol.* **57**, 242–247.
- Kenney, M. E., N. L. Oleinick, B. D. Richter and Y.-S. Li (1996) Phthalocyanine photosensitizers for photodynamic therapy and methods for their use. U.S. Patent 5,484,778.
- Li, Y.-S. and M. E. Kenney (1998) Methods of syntheses of phthalocyanine compounds. U.S. Patent 5,763,602.
- He, J., H. E. Larkin, Y.-S. Li, B. D. Richter, S. I. A. Zaidi, M. A. J. Rodgers, H. Mukhtar, M. E. Kenney and N. L. Oleinick (1997) The synthesis, photophysical and photobiological properties and in vitro structure-activity relationships of a set of silicon phthalocyanines PDT photosensitizers. *Photochem. Photobiol.* **65**, 581–586.
- Anula, H. M., J. C. Berlin, H. Wu, Y.-S. Li, X. Peng, M. E. Kenney and M. A. J. Rodgers (2006) Synthesis and photophysical properties of silicon phthalocyanines with axial siloxy ligands bearing alkylamine termini. *J. Phys. Chem. A* **110**, 5215–5223.
- Zhao, X. J., S. Lustigman, M. E. Kenney and E. Ben-Hur (1997) Structure-activity and mechanism studies on silicon phthalocyanines with plasmodium falciparum in the dark and under red light. *Photochem. Photobiol.* **66**, 282–287.
- Berlin, J. C. (2006) Silicon phthalocyanines for photodynamic therapy. Doctoral thesis, Case Western Reserve University.
- Lou, Y., X. Chen, A. C. S. Samia and C. Burda (2003) Femtosecond spectroscopic investigation of the carrier lifetimes in Dig-enite quantum dots and discrimination of the electron and hole dynamics via ultrafast interfacial electron transfer. *J. Phys. Chem. B* **107**, 12431–12437.
- Dayal, S., R. Krolicki, Y. Lou, X. Qiu, J. C. Berlin, M. E. Kenney and C. Burda (2006) Femtosecond time-resolved energy transfer from CdSe nanoparticles to phthalocyanines. *App. Phys. B* **84**, 309–315.
- Förster, Th. (1948) Intermolecular energy migration and fluorescence. *Ann. Phys.* **2**, 55–75.